

Karyotypic Complexity of the NCI-60 Drug-Screening Panel

Anna V. Roschke,¹ Giovanni Tonon,¹ Kristen S. Gehlhaus,¹ Nicolas McTyre,¹ Kimberly J. Bussey,² Samir Lababidi,² Dominic A. Scudiero,³ John N. Weinstein,² and Ilan R. Kirsch¹

¹Genetics Branch, and ²Laboratory of Molecular Pharmacology, Center for Cancer Research, National Cancer Institute, Bethesda, and ³Science Applications International Corporation-National Cancer Institute-Frederick Cancer Research and Development Center, Frederick, Maryland

ABSTRACT

We used spectral karyotyping to provide a detailed analysis of karyotypic aberrations in the diverse group of cancer cell lines established by the National Cancer Institute for the purpose of anticancer drug discovery. Along with the karyotypic description of these cell lines we defined and studied karyotypic complexity and heterogeneity (metaphase-to-metaphase variations) based on three separate components of genomic anatomy: (a) ploidy; (b) numerical changes; and (c) structural rearrangements. A wide variation in these parameters was evident in these cell lines, and different association patterns between them were revealed. Analysis of the breakpoints and other specific features of chromosomal changes across the entire set of cell lines or within particular lineages pointed to a striking lability of centromeric regions that distinguishes the epithelial tumor cell lines. We have also found that balanced translocations are as frequent in absolute number within the cell lines derived from solid as from hematopoietic tumors. Important similarities were noticed between karyotypic changes in cancer cell lines and that seen in primary tumors. This dataset offers insights into the causes and consequences of the destabilizing events and chromosomal instability that may occur during tumor development and progression. It also provides a foundation for investigating associations between structural genome anatomy and cancer molecular markers and targets, gene expression, gene dosage, and resistance or sensitivity to tens of thousands of molecular compounds.

INTRODUCTION

The “NCI-60” cell lines were developed by the National Cancer Institute for *in vitro* anticancer drug screening (1–5). The cell lines reflect diverse cell lineages [lung, renal, colorectal, ovarian, breast, prostate, central nervous system (CNS), melanoma, and hematological malignancies]. Since 1990, data on drug-related cytotoxicity for >100,000 compounds have been collected. In addition, many genes that have been causally investigated or frankly implicated in tumorigenesis and cancer progression (molecular targets) have been studied, at the DNA, RNA, and protein level [p53, mismatch repair (MMR) status, cell cycle checkpoints, and so forth], and expression analysis of >8000 genes performed (3, 6–12).⁴

We used spectral karyotyping (SKY) to provide a refined description of the chromosomal complement of these cell lines. Most of them had not been karyotyped since the late 1980s when cytogenetic techniques were significantly less powerful and informative. This comprehensive cytogenetic analysis included delineation of chromosomal abnormalities, and identification of karyotypic patterns and distinctive karyotypic features to facilitate integration of these data with other extant databases (gene expression, molecular targets, drug resistance and sensitivity) for the same cancer cell line panel.

Received 6/5/03; revised 9/30/03; accepted 10/17/03.

The costs of publication of this article were defrayed in part by the payment of page charges. This article must therefore be hereby marked *advertisement* in accordance with 18 U.S.C. Section 1734 solely to indicate this fact.

Notes: Drs. Roschke and Tonon contributed equally to this work. Supplemental data relating to this article may be found at www.aacr.org.

Requests for reprints: Ilan Kirsch, Genetics Branch, Center for Cancer Research, National Cancer Institute, National Naval Medical Center, 8901 Wisconsin Avenue, Building 8, Room 5101, Bethesda, MD 20889-5105. Phone: (301) 402-6382; Fax: (301) 496-0047; E-mail: kirsch@exchange.nih.gov.

⁴Internet addresses: <http://dtp.nci.nih.gov> and <http://discover.nci.nih.gov>

MATERIALS AND METHODS

Cell Lines. Fifty-nine cell lines from the NCI-60 anticancer drug discovery panel were obtained from Richard Camalier of the National Cancer Institute Developmental Therapeutics Program. Cells were grown in RPMI 1640 supplemented with 10% fetal bovine serum and 5 mM L-glutamine. Cell lines were harvested for metaphase chromosomes by mitotic shake-off after Colcemid treatment (0.025 μ g/ml; 1–3 h). They were then processed by standard cytogenetic methods using 0.075 M KCl and methanol-acetic acid (3:1) fixative (13). Metaphase spreads were prepared under optimized humidity conditions using a Thermotron cytogenetic drying chamber (Thermotron Industries, Holland, MI).

SKY. The SKY hybridization protocol has been described in detail (14, 15). Chromosome-specific painting probes were generated in our laboratory from chromosome-specific template DNA (kindly provided by Dr. Thomas Ried, Center for Cancer Research, National Cancer Institute, Bethesda, MD) using two consecutive rounds of degenerate oligonucleotide-primed PCR. Chromosome labeling was performed by incorporating Rhodamine 110-dUTP (Perkin-Elmer, Foster City, CA), Spectrum Orange-dUTP, Texas Red-dUTP (Molecular Probes, Eugene, OR), biotin-16-dUTP, and digoxigenin-11-dUTP (Boehringer Mannheim, Indianapolis, IN) in a secondary PCR reaction. Combinatorial fluorescence was produced by combining differentially labeled chromosome painting probes (14). The biotinylated probe sequences were visualized using Avidin-Cy5 (Amersham, Piscataway, NJ), and the digoxigenin-labeled probe sequences by incubation with mouse antidigoxigenin antibody (Sigma, St. Louis, MO) after sheep antimouse-antibody conjugated to Cy5.5 (Amersham).

Image acquisition was performed using an SD200 Spectracube (Applied Spectral Imaging, Carlsbad, CA) mounted on a Leica DMRXA microscope (Leica, Wetzlar, Germany) through a custom designed optical filter (SKY v.3; Chroma Technology, Brattleboro, VT). Applied Spectral Imaging software (Spectral Imaging and SkyView) was used for image acquisition and analysis. Breakpoints on the SKY-painted chromosomes were determined by comparison with corresponding inverted 4',6-diamidino-2-phenylindole banding of the same chromosome and by comparison with the G-banded karyotype of the same cell line.

Ten metaphases were analyzed for each cell line. Results were reported using the short form of the International System for Human Cytogenetic Nomenclature (ISCN; Ref. 16). Chromosomal aberrations were considered as clonal if found in two or more metaphases of the same cell line (in three or more metaphases for chromosome loss), according to ISCN conventions. Aberrations found in only one metaphase were designated as uncommon or “nonclonal.” On the basis of all of the clonal aberrations found in all of the analyzed metaphases, we created a composite karyotype for each cell line.

Fluorescence *in situ* hybridization (FISH) on CCRF-CEM was performed as described (17), using a probe specific for the telomeric end of the chromosome 9 p arm (Vysis, Downers Grove, IL).

G-Banding. G-banding of the NCI-60 panel of cell lines was performed on a contract basis by Hazleton Biotechnologies (Kensington, MD) and Children’s Hospital of Michigan (Detroit, MI) between 1985 and 1992.

Internet Resources. The complete karyotypes for 59 cell lines can be viewed on the Internet.⁵ Representative images of karyotypes in classification colors were edited through a pixel-to-vector image conversion procedure. An ISCN karyotype description accompanies each image.

The karyotypes can also be viewed on the SKY/comparative genomic hybridization database website.⁶ This database is a part of the Cancer Chromosome Aberration Project sponsored by the National Cancer Institute (18).

⁵Internet address: <http://home.ncicrf.gov/CCR/60SKY/new/demo1.asp>

⁶Internet address: <http://www.ncbi.nlm.nih.gov/sky/skyweb.cgi>

Statistical Analysis. Detailed information on all of the statistical methods and results is in the Supplementary Data. Simple descriptive statistics were used to summarize the associations between the variables: modal chromosome number, numerical complexity, numerical heterogeneity, structural complexity, and structural heterogeneity. We tested the null hypothesis that the correlation coefficient is equal to zero. However, for the mean number of translocations and deletions, bootstrap 95% confidence interval for the Pearson's correlation coefficient was calculated. Numerical and structural complexity and heterogeneity were tested between the two levels for the variable MMR status using exact test for Wilcoxon rank sum statistic, and the means of numerical and structural complexity were tested between the presence and absence of P53 mutation (P53) using asymptotic two-sample *t* test. The levels of retinoblastoma (Rb) protein were tested between two cell line groups, presenting or not presenting chromosome 13 loss (two cell lines showing a gain of chromosome 13 were excluded from this analysis) using Wilcoxon rank sum test.

To detect nonrandom occurrences of chromosome breakpoints in each of a set of 107 bands we devised a one-sided statistical test based on the Poisson distribution. Under the appropriate assumptions, the number of breakpoints in a given band $\Lambda_{i,j}$ follows a Poisson distribution with mean $\theta_{i,j}$, for each one of the 58 cell lines in each band, where $i = 1, \dots, 58$ and $j = 1, \dots, 107$. By estimating the individual means from the data we tested the null hypothesis $H_0: \Lambda_{i,j} = \theta_{i,j}$ against the alternative $H_a: \Lambda_{i,j} > \theta_{i,j}$ using the sum statistic Λ_j with mean θ_j , where

$$\theta_j = \frac{l_j}{L} N,$$

l_j is the size of the band, L is the total chromosome length, and N is the total number of breakpoints. The P was then defined as

$$P = \text{Prob}(\Lambda_j > \lambda_j), \text{ if } \lambda_j < \theta_j,$$

given that the null hypothesis H_0 is true.

To control for the overall type I error in the experiment so that the probability of declaring any of the 107 tests to be represented nonrandomly does not exceed the 0.05 bound, we additionally used the Bonferroni-Holm step-down multiple comparison procedure on the P s calculated above. Similar calculations were performed for the number of breakpoints in the centromeric regions only without accounting for the other bands for all of the chromosomes except the Y chromosome, using, again, a right-sided test. This resulted in 11 univariate hypothesis tests.

Right-sided Fisher's exact test was used to test the hypothesis of whether the number of abnormalities in a particular tissue is more than the number of abnormalities in the rest of the tissues. Similar testing was performed for the centromeric bands but using left-sided exact binomial test.

RESULTS

Our study involved multiple levels of data analysis. At the first level we make available the composite karyotypes both pictorially and in written format. At the second level, karyotypic complexity is described. At the third level, heterogeneity of the cell lines is analyzed. Level four involves the delineation of some of the specific features of numerical or structural changes across the entire set of cell lines or within those of particular lineages. Finally, we demonstrate how it is possible to start to integrate these data with other established features of these cell lines such as MMR, P53, and Rb status.

Karyotypes of the NCI-60

We performed spectral karyotypic analysis on 59 cancer cell lines from the NCI-60 panel (MDA-N cell line was unavailable because of restricted access). We found that karyotypes of 58 cell lines were unrelated to each other, but one line (MDA-MB-ADR), which had been originally considered a derivative of MCF-7, was actually a derivative of OVCAR-8 (data not shown). ISCN descriptions of

each cell line together with a representative image or ideogram are available.^{5,6}

Complexity of Karyotypes

Every cell line in the NCI-60 panel had karyotypic abnormalities, but there were notable individual variations among the cell lines in the level of karyotypic complexity. We defined the complexity of the karyotype based on the basis of three factors: ploidy changes, numerical abnormalities, and structural rearrangements.

Ploidy. Evaluation of ploidy for each cell line was based on the determination of the modal chromosome number and the range of the total number of chromosomes per metaphase. On the basis of the ISCN (16), if a cell line presented with a chromosome modal number between 35 and 57, it was considered near-diploid; if the chromosome modal number was between 58 and 80, near-triploid; if between 81 and 103 near-tetraploid, and between 104 and 126 near pentaploid. Twenty-three cell lines were identified as near-diploid, 22 as near-triploid, 13 as near-tetraploid, and 1 as near-pentaploid (Table 1). There was essentially a continuum of cell lines from near-diploid to near-triploid. Almost half of the cell lines had chromosome counts in the hyperdiploid/hypotriploid range (Fig. 1).

Numerical Complexity. Numerical chromosomal complexity was expressed in relation to the cell line ploidy level according to ISCN convention (16). Gains were counted as clonal if they occurred in at least two metaphases, whereas losses were counted as clonal if they occurred in at least three metaphases (16). This evaluation of numerical chromosome changes is summarized in Table 1, Column "N" (for numerical). Only one cell line (HCT15) had no numerical abnormalities. For all of the other cell lines, the range of numerical changes ranged from 1 to 28. The number of numerical changes correlated positively with the modal chromosome number ($r=0.73$; $P < 0.0001$), but there were numerous exceptions (Fig. 1). For instance, some near-diploid lines (NCI-H322M and NCI-H522) have a high level of numerical changes, whereas some near-tetraploid lines (SKOV-3 and MOLT-4) had relatively few numerical changes.

Structural Complexity. Chromosomes were counted as structurally abnormal if they contained translocations, deletions, duplications, insertions, inversions, or homogeneously staining regions. Identical rearrangements present in two or more metaphases were designated as clonal; rearrangements present in only one metaphase were designated as nonclonal or uncommon.

Every cell line in the NCI-60 panel showed at least one structural chromosomal rearrangement. Renal carcinoma cell line ACHN had just one clonal rearrangement. The lung cancer cell line NCI-H322M had the most, 45 [Table 1, column "S" (for structural); Fig. 2B]. Structural complexity of karyotypes had a weak but significant association with the modal chromosome number ($r = 0.28$; $P = 0.036$; Fig. 1). A statistically significant but not strong correlation found between structural and numerical complexity of karyotypes ($r = 0.48$; $P = 0.0002$) suggests that, in some cases, these two parameters may be related, but unrelated in others (Fig. 1).

Heterogeneity of Karyotypes

We defined "heterogeneity" as metaphase-to-metaphase variations present in the karyotype of a given cell line. We detected several types of karyotypic variability: (a) variation in ploidy level (ploidy heterogeneity); (b) variation in the number of given chromosome (numerical heterogeneity); and (c) the presence of nonclonal, structurally abnormal chromosomes (structural heterogeneity).

Ploidy Heterogeneity. Ploidy heterogeneity was characterized on the basis of SKY and previously obtained G-banding. G-

Table 1 Ploidy, structural, and numerical karyotypic complexity

Origin	Ploidy																
	±2n	M ^a	S	N	±3n	M	S	N	±4n	M	S	N	±5n	M	S	N	
Hematopoietic	CCRF-CEM	48	2	1	K562	65	15	11	MOLT-4	94	4	7					
	SR	46	4	1	RPMI-8226	64	22	12									
	HL-60(TB)	45	7	3													
Colon	HCT-15	44	4	0	COLO205	72	14	17									
	HCT-116	45	5	1	HT29	67	16	10									
	HCC-2998	44	6	3													
	KM12	43	7	8													
	SW-620	49	16	3													
Lung	NCI-H522	51	9	11	NCI-H226	62	17	16	HOP-62	103	19	28					
	NCI-H460	53	8	7	A549/ATCC	62	5	10	HOP-92	94	28	25					
	NCI-H322M	47	45	17	EKVX	62	27	13									
	NCI-H23	57	28	12													
Renal	ACHN	51	1	8	CAKI-1	67	11	11	786-0	83	8	20					
	UO-31	46	4	5	A498	74	14	18	TK-10	81	14	18					
					RXF-393	58	19	16									
					SN12C	64	28	18									
Breast	T-47D	57	17	12	BT-549	70	12	13									
	MDA-MB-231	54	22	14	HSS578T	57	24	14									
	MDA-MB-435	57	24	11	MCF7	65	38	12									
Ovarian	OVCAR-5	54	15	11	OVCAR-4	70	35	13	IGROV1	85	9	9					
	OVCAR-8	56	40	15	OVCAR-3	69	35	13	SKOV-3	84	17	6					
Prostate Melanoma					DU-145	59	17	11	PC-3	87	30	14					
					UACC-62	73	9	9	MALME-3M	82	7	17					
					UACC-257	70	9	12	SK-MEL-2	82	16	25					
					LOX IMVI	64	11	12	SK-MEL-5	100	16	27					
					M14	60	12	10	SK-MEL-28	88	26	17					
CNS	SNB-75	55	4	12	SNB-19	61	9	12	SF-539	88	29	19	SF-295	116	14	24	
	U251	52	20	8													
	SF-268	56	22	7													

^a M, modal chromosomal number; N, number of numerical changes; S, number of clonal, structurally rearranged chromosomes.

banding, performed for the NCI-60 between 1985 and 1992 (see "Materials and Methods"), did not allow a precise delineation of the karyotypic abnormalities for the majority of cell lines, but chromosome counts were obtained on 100 metaphases for 52 cell lines (data not shown). According to this G-banding data, only one cell line (SR) had no variations in ploidy. In 29 cell lines, the ploidy level differed in 1–10% of the cells analyzed. For 23 of the lines, >10% of the cells had a ploidy different from that of the major population. For example, if the majority of cells had a near-diploid karyotype, there might be an additional small popu-

lation of cells with a near-tetraploid chromosome count. Near-triploid cell lines usually had small additional populations of cells with a near-pentaploid or near-hexaploid count, or, in few cases, with a near-diploid count.

On the basis of our SKY analysis of 10 cells per cell line, we also found ploidy heterogeneity in 24 of the 59 lines (data not shown). Despite the relatively few metaphases analyzed, we were able to identify ploidy heterogeneity in the same subgroup of the cell lines that had shown the most ploidy heterogeneity in the previous G-banding based analysis.

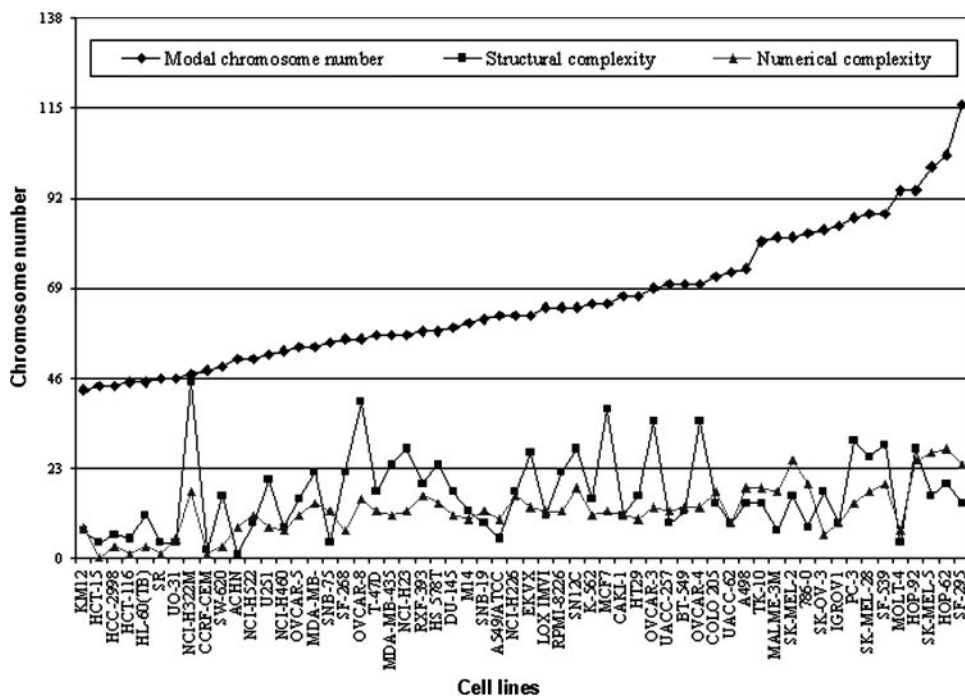


Fig. 1. Structural and numerical complexity of karyotypes of the NCI-60 cell lines. Numbers of structurally and numerically abnormal chromosomes for every cell line are aligned according total (modal) chromosome numbers. Numerical complexity positively correlated with modal chromosome number ($r = 0.73$; $P < 0.0001$). Structural complexity had weak but statistically significant correlation with modal chromosome number ($r = 0.28$; $P = 0.036$). Structural and numerical complexity had statistically significant correlation ($r = 0.48$; $P = 0.0002$).

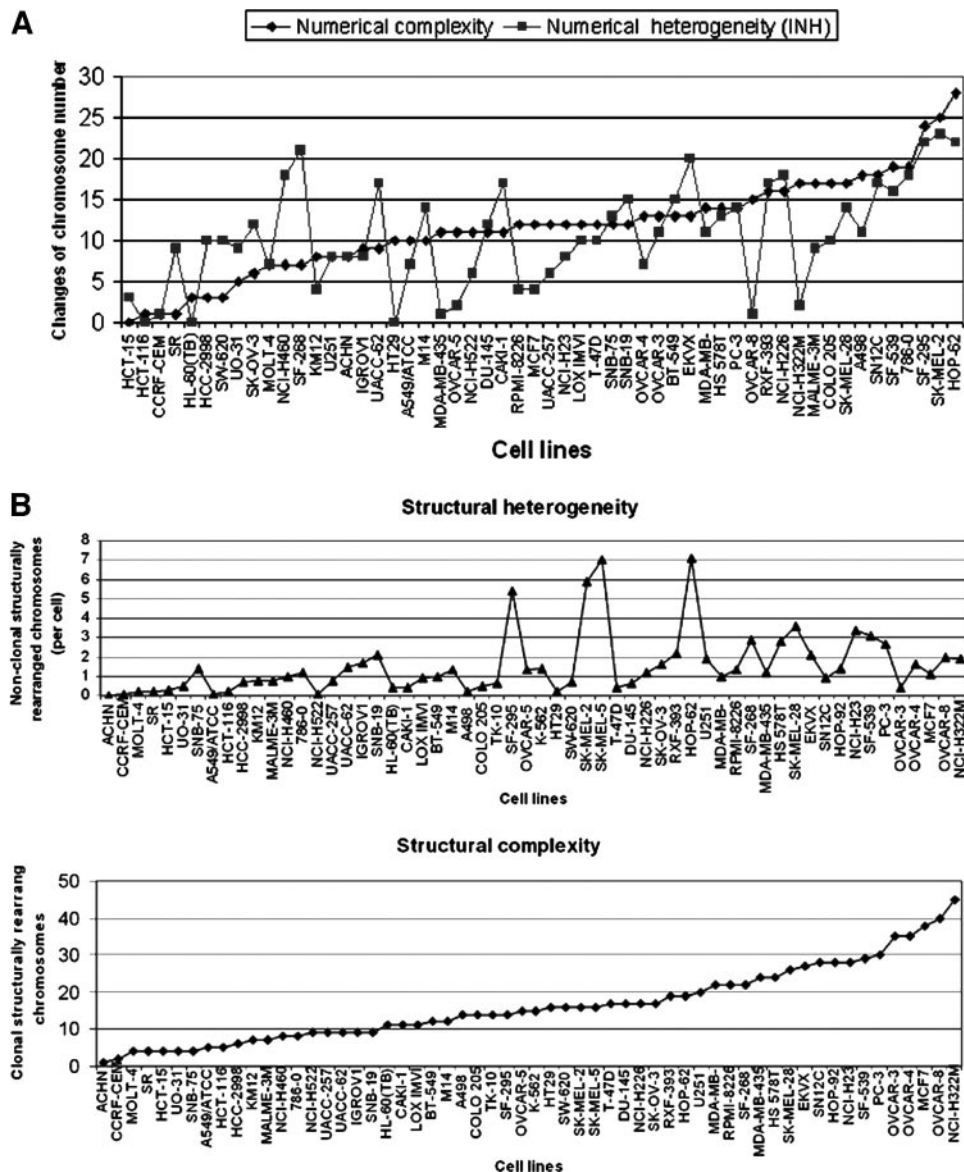


Fig. 2. A, numerical heterogeneity versus numerical complexity of the NCI-60 karyotypes. Index of numerical heterogeneity (INH) was calculated as a number of chromosomes with numerical variability. Both normal and derivative chromosomes were included in analysis. There was a correlation between INH and numerical complexity (Pearson's correlation coefficient 0.60; $P < 0.0001$). B, structural heterogeneity versus structural complexity of karyotypes. Structural heterogeneity was estimated as the number of nonclonal structural rearrangements per metaphase. Structural heterogeneity had statistically significant correlation with structural complexity (Spearman's correlation coefficient 0.57; $P < 0.0001$).

The cell lines with the most ploidy variation were SK-MEL-2, SK-MEL-5, SF-539, PC-3, and TK-10.

Numerical Heterogeneity. Chromosomal changes present in only a fraction of cells were considered to indicate numerical heterogeneity. "Numerical heterogeneity" means that in different metaphases of the same cell line a different number of similar chromosomes can be present. Two types of "similarity" were used to group chromosomes: (a) the same centromere; and (b) the same normal or structurally abnormal chromosome. Accordingly, numerical heterogeneity was first assessed based on the presence of metaphase-to-metaphase variation in the number of like centromeres. Loss of a centromere in two cells or gain in only one cell was not counted because of the possibility of mechanical loss or gain during preparation of the metaphase spreads. Any centromere type showing a higher number of gains or losses was considered as variable, and tallied as "one point" in what we define as an "index of numerical heterogeneity" (INH). Fig. 2A shows the distribution of this INH among the NCI-60 cell lines. Because X and Y centromeres were grouped together, the INH cannot be >23.

Grouping of like centromeres does not identify differential gains or losses of a normal or structurally abnormal chromosome that contain

the same centromere. Therefore, for each cell line we calculated the fraction of normal chromosomes that experience numerical heterogeneity and the fraction of abnormal chromosomes that showed numerical heterogeneity. The data for this analysis are shown in Table 2.

In general, the overall level of numerical heterogeneity for the entire chromosome complement of a given cell line was consistent with the level of numerical variability of either the normal or structurally abnormal chromosomes present in that cell line. However, exceptions occurred. For example, NCI-H226 had a large fraction of normal chromosomes (17 of 23 or 0.74) that experienced numerical heterogeneity, whereas a much smaller fraction of structurally abnormal chromosomes (3 of 17 or 0.17) experienced numerical heterogeneity (Table 2). Several other cell lines (A549, HOP-62, SNB-19, SF-295, COLO 205, CAKI-1, and DU-145) showed this same trend. In contrast, in some other cell lines (NCI-H322M, HCC-2998, and MCF7) normal chromosomes showed less numerical heterogeneity than did structurally abnormal ones. Thus, in some cell lines normal and structurally aberrant chromosomes were equally unstable, whereas in others one or the other group showed relative stability.

Structural Heterogeneity. Structural heterogeneity was estimated as the number of nonclonal structurally abnormal chromosomes per

Table 2 Fraction of numerically heterogeneous chromosomes among normal and structurally aberrant chromosomes

Cell lines	Tissue	Normal ^a	Aberrant ^b
NCI-H23	Lung	0.56	0.78
NCI-H226	Lung	0.74	0.17
NCI-H322M	Lung	0.39	0.73
NCI-H460	Lung	0.82	0.50
NCI-H522	Lung	0.48	0.34
A549/ATCC	Lung	0.56	0.20
HOP-62	Lung	0.87	0.36
EKVX	Lung	0.66	0.88
OVCAR-3	Ovarian	0.48	0.66
OVCAR-4	Ovarian	0.30	0.34
OVCAR-5	Ovarian	0.08	0.15
OVCAR-8	Ovarian	0.00	0.08
IGROV1	Ovarian	0.48	0.67
SK-OV-3	Ovarian	0.43	0.25
SNB-19	CNS	0.65	0.34
SNB-75	CNS	0.61	0.75
U251	CNS	0.43	0.75
SF-268	CNS	0.74	0.63
SF-295	CNS	0.95	0.50
SF-539	CNS	0.74	0.41
CCRF-CEM	Leukemia	0.00	0.00
MOLT-4	Leukemia	0.30	0.00
HL-60(TB)	Leukemia	0.00	0.00
SR	Leukemia	0.22	0.25
RPMI-8226	MM	0.22	0.23
HT29	Colon	0.00	0.00
HCC-2998	Colon	0.34	0.83
HCT-116	Colon	0.00	0.00
SW-620	Colon	0.43	0.50
COLO 205	Colon	0.56	0.21
HCT-15	Colon	0.13	0.00
KM12	Colon	0.22	0.43
UO-31	Renal	0.34	0.25
SN12C	Renal	0.52	0.50
A498	Renal	0.65	0.50
CAKI-1	Renal	0.82	0.36
RXF-393	Renal	0.66	0.52
ACHN	Renal	0.30	0.00
786-0	Renal	0.66	0.50
LOX IMVI	Melanoma	0.43	0.64
MALME-3M	Melanoma	0.52	0.29
SK-MEL-2	Melanoma	1.00	0.75
SK-MEL-28	Melanoma	0.61	0.65
UACC-62	Melanoma	0.78	0.77
UACC-257	Melanoma	0.61	0.44
M14	Melanoma	0.52	0.42
MCF7	Breast	0.08	0.34
HS 578T	Breast	0.56	0.79
MDA-MB-435	Breast	0.08	0.21
MDA-MB-231/ATCC	Breast	0.34	0.24
BT-549	Breast	0.74	0.58
T-47D	Breast	0.34	0.35
DU-145	Prostate	0.61	0.29
PC-3	Prostate	0.82	0.63

^a Fraction of numerically heterogeneous chromosomes among normal chromosomes: $\frac{\text{number of normal numerically heterogeneous chromosomes}}{23}$.

^b Fraction of numerically heterogeneous chromosomes among structurally abnormal chromosomes: $\frac{\text{number of structurally abnormal numerically heterogeneous chromosomes}}{\text{total number of different structurally abnormal chromosomes}}$.

metaphase. For example, if among 10 analyzed metaphases 5 different nonclonal structurally rearranged chromosomes were found, the structural heterogeneity would be calculated as $5/10 = 0.5$ nonclonal structurally rearranged chromosomes per metaphase.

The level of heterogeneity may indicate ongoing chromosomal instability and allow assessment of its role in karyotypic evolution. This suggestion is validated by our previous experiments, in which the level of structural heterogeneity in single cell subclones of four of these same cell lines (HCT-116, HT-29, SKOV-3, and OVCAR-8) was determined after their propagation in culture (15). This value was found to be consistent with the “snapshot” value obtained by an analysis of 10 metaphases from each of those cell lines, as described above.

No SH was detected in 1 cell line, ACHN, in which no nonclonal structural rearrangements were found. The level of structural heterogeneity was relatively low (less than one nonclonal rearrangement per metaphase) in 27 cell lines. Nineteen cell lines had from 1 to 2 nonclonal, structurally abnormal chromosomes per metaphase. Seven cell lines had from 2 to 3 nonclonal, structurally abnormal chromosomes per metaphase, and 4 cell lines had >4 (Fig. 2B).

Interestingly, structurally “stable” cell lines were found among those with both structurally simple and complex karyotypes. Structural instability was seen in some karyotypically simple cell lines. In general, the karyotypically “simple” cell lines showed less structural heterogeneity than did cell lines with complex karyotypes. However, the most structurally heterogeneous cell lines were found among those with karyotypes that were neither the least nor the most structurally rearranged (HOP-62, SKMEL-2, SKMEL-5, and SF-295).

Both structural and numerical heterogeneity positively correlated with the modal chromosome number (Spearman’s correlation coefficient = 0.40, $P = 0.002$, and Pearson’s correlation coefficient = 0.51, $P < 0.0001$, respectively).

Specific Numerical and Structural Changes

Recurrent Numerical Changes. Numerical changes were expressed in relation to the cell line-specific ploidy level, and according to ISCN convention, included normal as well as derivative chromosomes in the count. Therefore, “chromosome copy number” in this analysis actually reflects most accurately the number of like centromeres.

Common and tissue-specific recurrent numerical changes are summarized in Table 3. The most frequent autosomal numerical changes across the whole NCI-60 panel were, in order: -13 , $+7$, $+5$, $+20$, -21 , and -22 . Chromosome Y had been lost partially or completely in 13 of the 29 cell lines known to be of male origin. Individual tissue-specific changes included gain of chromosome 12 in lung cancer cell lines, gain of chromosome X in CNS cell lines, and loss of chromosome 6 in renal carcinoma cell lines. Specific combinations of the most frequent gains and losses were also found for every tissue type (Table 3).

Because the chromosome 13 centromeric region was one of the most frequently lost in this panel of cell lines, we additionally investigated the nature of chromosome 13 numerical and structural changes (Table 1 of Supplemental Data). The underlying goals of this analysis were to define the critical features of chromosome 13 of which the loss might be essential to carcinogenesis and to determine how given cancer cells accomplished that loss. Results of the analysis are described in the Supplemental Data.

Structural Abnormalities. There was a great diversity of structural chromosomal abnormalities in the NCI-60 cell line panel. We detected the following structural rearrangements: translocations, deletions, homogeneously staining regions (HSR), inversions, duplications, insertions, acentric fragments, minutes, and double minutes (Table 4). Translocations and deletions were among the most frequent rearrangements. In total, we found 817 clonal translocations and 245 clonal deletions in 58 independent cell lines. Among the nonclonal rearrangements, translocations and deletions also prevailed; 551 translocations and 187 deletions were detected.

Translocations were found in every NCI-60 cell line and every chromosome experienced translocations. The most “translocation-rich” cell lines were of ovarian, prostate, lung, and breast lineages (Table 5). Leukemia/lymphoma and colon cancer cell lines had the least number of translocations per cell line.

Deletions were present in all but 1 cell line (ACHN). Ovarian, breast, and CNS cell lines had the highest number of deletions per cell

Table 3 Recurrent gains and losses of chromosomes in the NCI-60 panel of cancer cell lines

Chromosome no.	Gained ^a	Lost ^a	Lung ^b	Ovarian ^b	Central nervous system ^b	Colon ^b	Renal ^b	Melanoma ^b	Breast ^b	Prostate ^{b,c}	Leukemia ^b
1	20	9		+1			+1				
2	21	9	+2				+2	+2			
3	18	11			+3			+3		-3	
4	6	28		-4	-4		-4	-4			
5	34	6	+5			+5	+5		+5	+5	
6	15	15				+6	-6				
7	34	4	+7		+7	+7	+7	+7	+7		
8	18	15				+8			+8		
9	14	17						-9	+9		
10	7	23			-10			-10			-10
11	16	16	-11		+11	+11		-11			
12	16	16	+12								
13	3	35	-13	-13	-13	-13	-13	-13	-13	-13	
14	6	27			-14		-14	-14	-14		-14
15	13	20				+15	-15		-15	-15	
16	16	19						-16		-16	
17	15	15									
18	8	21			-18	-18		-18			
19	11	21					-19		-19		
20	33	8		+20	+20	+20		+20	+20		
21	10	32	-21			-21		-21		-21	
22	8	31	-22			-22	-22			-22	
X	13	16		-X	+X		-X		-X		-X
Y	2	13			-Y	-Y	-Y	-Y			

Gains and losses found in >50% of cell lines of particular origin are printed in bold font, and consistent numerical changes found in 20–50% of cell lines are printed in plain font.

^a Total number of chromosomal gains and losses in 58 independent cell lines.

^b Tissue-specific gains and losses.

^c NCI-60 panel includes only two prostate cancer cell lines.

Table 4 Structural rearrangements found in the NCI60 cancer cell line panel

	Clonal	Nonclonal
Translocations	817	551
Deletions	245	187
Inversions	9	0
Insertions	5	0
Duplications	20	0
HSR	12	4

line, whereas leukemia/lymphoma, colon, and renal cell lines presented the lowest number (Table 5).

Breakpoints Analysis. Breakpoints analysis was performed for all identified clonal rearrangements. More than 95% of analyzed breakpoints originated from translocations and deletions. To determine whether breakpoints occurred nonrandomly, we calculated Poisson P s for the number of breakpoints in each region, except the bands p11-q11 surrounding the centromeric region and chromosome Y. These P s were additionally corrected using Bonferroni-Holm Step-Down multiple comparison procedure to control for the overall type I error. Only the regions that presented a higher than expected involvement were included in the analysis (see “Materials and Methods” and Supplemental Data).

Centromeric regions were the most frequently involved in chromosomal rearrangements (Fig. 3). In fact, among clonal translocations with identified breakpoint regions (765 translocations), 406 involved the centromeric region (53.1%), and 127 involved the terminal bands of chromosomes (16.6%). The group of clonal translocations at centromeric regions included mainly centromeric-centromeric interactions (277 translocations or 68.2%). Telomeric-centromeric fusions represented a smaller proportion of translocations: only 21 translocations or 5.1% of all of the centromeric translocations. Among 551 nonclonal translocations, centromeric regions were involved in 244. Only 43 translocations involved terminal bands.

Using corrected Poisson P s after applying the multiple comparison procedure, we found that chromosomes 5 and 1 had significantly more clonal centromeric breakpoints across all of the cell lines than the overall expected number (Table 3 of Supplemental Data).

The distribution of centromeric breakpoints among different chro-

mosomes was distinct for different cell line lineages. Some lineages showed a similar, highly significant pattern of centromeric involvement (colon and lung, for example; or renal and melanoma; Spearman Rho nonparametric correlation, $P < 0.001$; data not shown). On the basis of the exact binomial test we found that the proportion of the centromeric breakpoints in the lymphoma/leukemia cell lines was highly significantly less than expected ($P < 0.0001$).

We calculated the Poisson P s for all of the regions excluding the centromeric ones and chromosome Y. In five regions (3p21, 11q14, 1q12, 17q21, and 9p23) the number of breakpoints was significantly higher than expected after correcting for multiple comparison procedure at the 0.05 significance level (Table 2 of Supplemental Data). Additionally, 35 regions presented a statistically significant number of breakpoints before this correction was applied. Because the multiple comparisons procedure used in this analysis does not take into consideration a possible correlation that could exist between different regions and is very conservative, these regions should be regarded as potentially important (Table 2 of Supplemental Data).

To determine whether these bands, presenting a significant Poisson P , were involved in breakpoints preferentially in some tissues, we performed a right-sided Fisher’s exact test. Several bands were involved significantly more often in ovarian, breast, and colon than in other cell lines (Table 3 of Supplemental Data).

Hotspots of Rearrangements. We noticed that some breakpoints were involved in different rearrangements in the same cell line more

Table 5 Frequencies of clonal translocations and deletions

Cancer cell lines	Average number of translocations per cell line	Average number of deletions per cell line
Leukemia/lymphoma	5.0	1.2
Colon	7.7	2.6
Breast	18.5	6.8
Ovarian	26.0	7.2
Prostate	30.5	5.0
Lung	20.0	3.8
Renal	11.3	3.0
Melanoma	9.9	4.2
Central nervous system	11.7	5.8
Solid tumors	15.1	4.8

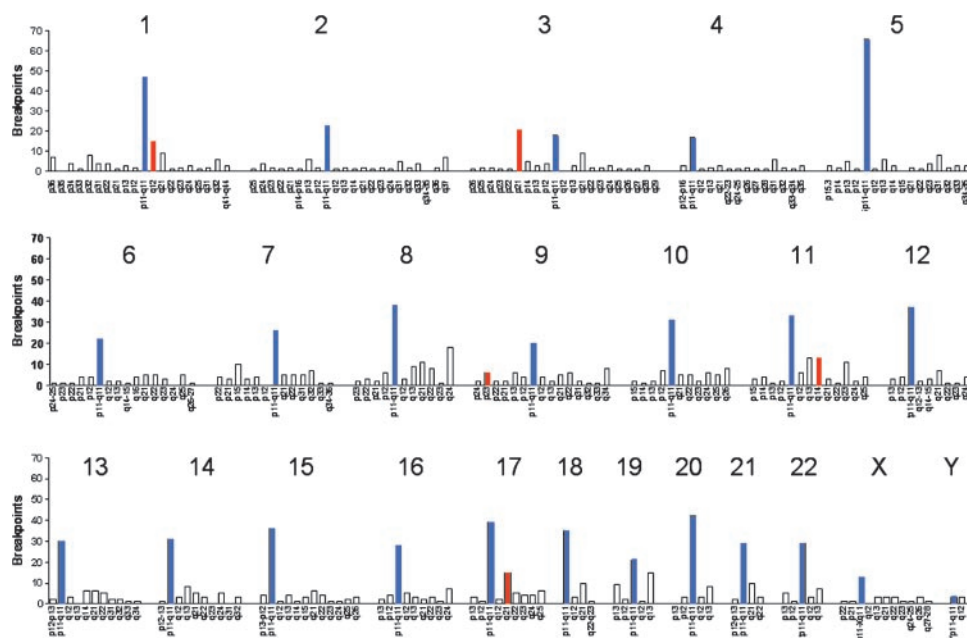


Fig. 3. Breakpoint distribution combining all of the cell lines. Centromeric regions are indicated in blue; bands that present more breakpoints than expected by chance, after the multiple comparison procedure (see “Materials and Methods” and Supplemental Data) are in red. Pericentromeric bands and chromosome Y were not included in the statistical analysis.

than once. These individual “hotspots” were detected in 36 cell lines, and the total number of hotspots was 234 (both clonal and nonclonal rearrangements were included in the hotspots analysis). Among them, 199 hotspots were found at centromeric regions of chromosomes, 5 at terminal bands, and 30 at intermediate bands (Table 4 of Supplemental Data). The most frequent hotspots included centromeric regions of chromosomes 5 (19 cell lines), 1 (18 cell lines), and 15 (14 cell lines). The least frequently involved centromeric hotspots were centromeric regions of chromosomes 16, 21, and X (4 cell lines each). Among noncentromeric bands, only 3p21 was a recurrent hotspot (in 2 cell lines).

The frequency of centromeric hotspots was different in different lineages. In leukemia cell lines no such hotspots were found (Table 6). Among solid tumor cell lines the average frequency of centromeric hotspots was 3.8 per cell line, with the lowest frequency in the colon cancer cell line group and the highest in the melanoma cell line group (Table 6). Therefore, both analyses of hotspots and breakpoints indicated that centromeric regions were notably less involved in rearrangements in leukemia cell lines than in solid tumor cell lines.

Balanced Reciprocal Translocations. The majority of translocations were unbalanced, but balanced, reciprocal translocations were also found. Among 817 clonal translocations in 58 independent cell lines, 24 translocations found in 20 cell lines were reciprocal and balanced with both derivatives clonally present. Three additional translocations were possibly reciprocal, because one derivative was present clonally, and the second was found “nonclonally” (*i.e.*, in only

1 of 10 metaphases), and 11 reciprocal translocations were nonclonal (Table 5 of Supplemental Data). The presence of nonclonal reciprocal derivatives matching clonal derivatives with translocations indicates that reciprocal translocations may occur even more frequently and appear as unbalanced translocations after the loss of one homologue.

Thus, 3% of translocations were identified as balanced. Perhaps surprisingly, we found that the frequency of cell lines with balanced translocations among leukemia cell lines and epithelial cancer cell lines was approximately the same (0.40 and 0.44 balanced translocations per cell line, respectively).

Almost every balanced translocation detected within the NCI-60 cell line panel was different, and involved different partners and breakpoints (Table 5 of Supplemental Data). Breakpoints 2q33, 6q25, and 9p23 participated in two different reciprocal translocations each. Translocation t(X;10)(q22~23; q25) was present in two breast cancer cell lines (clonal in BT549 and nonclonal in HS578T).

Jumping Translocations (JTs). The majority of clonal and nonclonal translocations were unbalanced (1307 translocations total). Among these translocations, 284 translocations (21.7%) were identified as JTs. JTs have been defined as nonreciprocal translocations involving a donor chromosome arm or chromosome segment fused to several different recipient chromosomes (19).

In the NCI-60 panel of cancer cell lines, 32 cell lines exhibited JTs involving from 1 to 24 different donor chromosome arms or segments per cell line. Table 6 (Supplemental Data) summarizes the donor and recipient chromosomes associated with each JT found in the NCI-60 panel of cancer cell lines. The most prevalent donors were 5p (20 JTs in 9 cell lines) and 15q (21 JTs in 7 cell lines).

Almost all of the donors and recipients consisted of the whole arms of chromosomes (Table 6 of Supplemental Data).

Isochromosomes. Isochromosomes represent a special kind of structural rearrangement involving centromeric fusion of two similar arms of a given chromosome or a misdivision of the centromere. Isochromosomes were found to be the most frequent recurrent aberrations in epithelial cancers (20, 21). Across the NCI-60 panel, 63 isochromosomes were detected in 30 cell lines. The most frequent isochromosomes were 5p (9 cell lines), 18p (6 cell lines), 8q and 15q (5 cell lines each), 5q and 13q (4 cell lines each), and 12q (3 cell lines).

Table 6 Frequencies of hotspots of structural rearrangements per cell line in different lineages

Cancer cell lines	Centromeric hotspots (per cell line)	Intermediate hotspots (per cell line)
Leukemia	0.0	0.4
Colon	1.0	0.4
Breast	3.2	1.5
Ovarian	2.7	0.7
Prostate	4.5	2.0
Lung	6.2	0.3
Renal	2.5	0.1
Melanoma	6.4	0.1
Central nervous system	3.5	0.5
Solid tumor	3.8	0.5

Among isochromosomes, 12 reciprocal pairs, or fissions, were found in 10 cell lines (9 clonal and 3 nonclonal; Table 5 of Supplemental Data). Three pairs among them had derivatives distributed into different cells.

Dicentrics. Dicentric chromosomes contain two centromeric regions. Fifteen clonal and 32 nonclonal dicentrics were found in 28 cell lines. Chromosome 14 was the most frequently involved in dicentric formation (10 cases). Among 15 clonal dicentrics, 5 were formed by telomeric associations; 4 had centromeric and 2 had intermediate band breakpoints. Intermediate-telomeric and intermediate-centromeric fusions were detected in 1 case each.

Associations of Karyotypic Parameters with MMR, P53, and Rb Status

Subclassifications of cancer cell lines based on their karyotypic complexity and heterogeneity provide a foundation for investigating associations between these parameters and numerous molecular markers and targets, gene expression, and gene dosage, as well as sensitivity or resistance to >100,000 independent chemical compounds already tested on these cell lines. As a starting point we looked at the distribution of MMR-defective cell lines among the NCI-60 cell line panel. MMR-defective cell lines are IGROV1 and SKOV3 (ovarian), HCT-116, HCT-15, and KM12 (colon), and CCRF-CEM (leukemia; Refs. 22, 23).⁷ We found that MMR-defective cell lines had less numerical and structural complexity than proficient cell lines ($P < 0.0001$ and $P = 0.011$, respectively; Wilcoxon test). Numerical heterogeneity was significantly less in the MMR-defective group than in MMR-proficient ($P = 0.0165$; Wilcoxon test), but SH was not significantly different ($P = 0.187$; Wilcoxon test).

We also looked at p53 status. Groups of p53 wild-type and p53 mutant cell lines include 18 and 38 cell lines, respectively (9). Structural but not numerical complexity was significantly lower in p53 wild-type cell lines compared with p53 mutants (structural: $P = 0.0126$; numerical: $P = 0.34$; two-sample t test).

Because chromosome 13 was the most frequently lost across the whole panel of cell lines, we asked about the relevance of this loss to Rb protein level. There was no significant difference in the Rb protein level between cell lines with or without a loss of chromosome 13 ($P = 0.24$; Mann-Whitney-Wilcoxon test).

DISCUSSION

Using the technique of SKY, we have delineated chromosomal rearrangements present in the cancer cell lines of the NCI-60 drug-discovery panel. The panel includes cancer cell lines of different lineages. Six of the cell lines represent malignancies of hematopoietic origin (5 leukemia/lymphoma lines and 1 multiple myeloma); 54 others represent different types of solid tumors. We obtained and analyzed 59 of the 60 cell lines and found that all of them were karyotypically abnormal. A wide spectrum of karyotypic abnormalities was detected. Representative karyotypes in classification colors for each cell line can be viewed along with their ISCN descriptions on the Internet.^{5,6} Karyotypes reported previously for some of these cell lines were highly similar in cases when SKY or multifluor-FISH was performed (15, 24–37). When previous karyotypes were obtained by G-banding,⁸ matches in a number of characteristic markers allowed us to conclude that the same cell lines had been analyzed but precise comparisons were not possible.

Complexity and Heterogeneity of Karyotypes. We studied three separate components of genomic structure: (a) ploidy; (b) numerical

variation of any particular chromosome from the base ploidy value; and (c) structural rearrangement. Analysis of karyotypic abnormalities present in the NCI-60 panel allowed us to describe specific recurrent aberrations and also to classify the cell lines on the basis of the complexity and heterogeneity of their karyotypic changes. Classification and subclassification of the cell lines provides a basis for their comparison, one with another and comparison as groups with other extant databases developed from this cell line resource (8, 11, 12).⁴ At the crudest level of comparison of karyotypic complexity, two predominant karyotypic patterns emerged: relatively simple, mostly near-diploid karyotypes and complex, usually hyperdiploid/near-triploid karyotypes. This dichotomy of karyotypes, in general, fits the existing description of neoplasia-associated karyotypic patterns (38, 39). Cell lines with near-tetraploid cell counts were found to have either high or low complexity.

Karyotypic heterogeneity was analyzed based on cell-to-cell variations in the karyotypic components. Heterogeneity was used as an indication of the presence or absence of ongoing chromosomal instability. On the basis of our observations, it is clear that at least three types of karyotypic instability operate in cancer cell lines: (a) instability at the ploidy level; (b) losses or gains of only certain chromosomes (numerical instability); and (c) structural chromosomal instability. These three kinds of instability lead to heterogeneity of the karyotypes of cancer cells and may provide a substrate for selection. Our earlier work suggests that, under steady-state culture conditions, only limited karyotypic evolution occurs, even in the presence of significant ongoing chromosomal instability (15). Stability of karyotypes over years of continuous cultivation has been reported for several well-studied cancer cell lines (27, 31, 40, 41). However, when culture conditions change (or a drug selection occurs), the presence of ongoing instability may provide the basis for selection and karyotypic change (42, 43).

As expected, most of the cell lines derived from hematopoietic malignancies had low levels of karyotypic complexity and heterogeneity (Table 7). Exceptions were cell lines K562 and RPMI-8226 (chronic myelogenous leukemia with blast crisis and multiple myeloma, respectively), which had the same level of karyotypic complexity as the majority of epithelial carcinomas. Most of colon, and few renal and lung cancer cell lines also were karyotypically simple (Table 7). Very high level of karyotypic complexity (>20 structurally or numerically rearranged chromosomes), often accompanied by a high level of structural and numerical heterogeneity, was found among lung, renal, breast, ovarian, prostate, skin, and CNS cancer cell lines.

Analysis of complexity and heterogeneity of chromosomal components revealed that there are diverse combinations of these parameters in cancer cell lines (Table 8). Different forms of chromosomal alterations often showed common trends and some linkage. This is consistent with a recent study of hamster cell lines (44). However, numerous exceptions were found suggesting that the destabilizing processes might be dependent on each other in some cases, but apparently independent in others.

Whereas intuition might suggest that complexity of karyotype is indicative of an ongoing process of genomic destabilization and that more complexity leads to more heterogeneity, there are many exceptions to this suggestion as well. For example, structurally stable cell lines were found among those with both structurally simple and more complex "signature" karyotypes (Table 8). The converse was also seen. Therefore, in some cases this suggests that the kind of instability that operated during the establishment of the signature karyotype is not still the operative one.

Different kinds of genetic instability are not mutually exclusive in cancer cell lines. For example, among the NCI-60 panel, microsatel-

⁷ B. Vogelstein, personal communication.

⁸ D. A. Scudiero, unpublished observations.

Table 7 *Karyotypic complexity and heterogeneity among the different lineages of the NCI-60 cell lines*

Cell lines	Tissue	Ploidy	SC ^a	NC	SH	NH
CCRF-CEM	Leukemia	2	Green	Green	Green	Green
MOLT-4	Leukemia	4	Green	Green	Green	Green
SR	Leukemia	2	Green	Green	Green	Green
HL-60(TB)	Leukemia	2	Green	Green	Green	Green
K-562	Leukemia	3	Green	Green	Green	Green
HCT-116	Colon	2	Green	Green	Green	Green
HCT-15	Colon	2	Green	Green	Green	Green
HCC-2998	Colon	2	Green	Green	Green	Green
KM12	Colon	2	Green	Green	Green	Green
SW-620	Colon	2	Green	Green	Green	Green
HT29	Colon	3	Green	Green	Green	Green
COLO 205	Colon	3	Green	Orange	Green	Green
ACHN	Renal	2	Green	Green	Green	Green
UO-31	Renal	2	Green	Green	Green	Green
CAKI-1	Renal	3	Green	Green	Green	Green
786-0	Renal	4	Green	Orange	Green	Green
A498	Renal	3	Green	Orange	Green	Green
TK-10	Renal	4	Green	Orange	Green	Green
RXF-393	Renal	3	Green	Orange	Green	Green
SN12C	Renal	3	Green	Orange	Green	Green
NCI-H460	Lung	2	Green	Green	Green	Green
NCI-H522	Lung	2	Green	Green	Green	Green
A549/ATCC	Lung	3	Green	Green	Green	Green
NCI-H226	Lung	3	Green	Green	Green	Green
NCI-H322M	Lung	2	Green	Orange	Green	Green
NCI-H23	Lung	2	Green	Orange	Green	Green
HOP-62	Lung	4	Green	Orange	Green	Green
EKVX	Lung	3	Green	Orange	Green	Green
HOP-92	Lung	4	Green	Orange	Green	Green
IGROV1	Ovarian	4	Green	Green	Green	Green
SK-OV-3	Ovarian	4	Green	Green	Green	Green
OVCAR-5	Ovarian	2	Green	Green	Green	Green
OVCAR-3	Ovarian	3	Green	Green	Green	Green
OVCAR-4	Ovarian	3	Green	Green	Green	Green
OVCAR-8	Ovarian	2	Green	Green	Green	Green
RPMI-8226	Myeloma	3	Green	Green	Green	Green
UACC-257	Melanoma	3	Green	Green	Green	Green
UACC-62	Melanoma	3	Green	Green	Green	Green
MALME-3M	Melanoma	4	Green	Orange	Green	Green
LOX IMVI	Melanoma	3	Green	Green	Green	Green
M14	Melanoma	3	Green	Green	Green	Green
SK-MEL-2	Melanoma	4	Green	Orange	Green	Green
SK-MEL-5	Melanoma	4	Green	Orange	Green	Green
SK-MEL-28	Melanoma	4	Green	Orange	Green	Green
T-47D	Breast	2	Green	Green	Green	Green
MDA-MB-435	Breast	2	Green	Green	Green	Green
MCF7	Breast	3	Green	Green	Green	Green
BT-549	Breast	3	Green	Green	Green	Green
MDA-MB-231/ATCC	Breast	2	Green	Green	Green	Green
HS 578T	Breast	3	Green	Green	Green	Green
DU-145	Prostate	3	Green	Green	Green	Green
PC-3	Prostate	4	Green	Green	Green	Green
SNB-75	CNS	2	Green	Green	Green	Green
SNB-19	CNS	3	Green	Green	Green	Green
U251	CNS	2	Green	Green	Green	Green
SF-268	CNS	2	Green	Green	Green	Green
SF-295	CNS	5	Green	Green	Green	Green
SF-539	CNS	4	Green	Green	Green	Green

^a SC, structural complexity; NC, numerical complexity; SH, structural heterogeneity; NH, numerical heterogeneity; CNS, central nervous system. Green, low level (the lower 33%); orange, high level (upper 33%); and gray, intermediate level of parameters.

lite instability coexisted with chromosomal instability; all of the microsatellite unstable cell lines showed rearranged karyotypes and indications of ongoing structural or numerical chromosomal instability. However, comparisons of MMR-deficient and proficient groups

of cell lines demonstrated that the level of structural and numerical complexity was, in general, lower in the cell lines that are MMR defective, as has been reported elsewhere (32). MMR-defective cell lines were among those cell lines that had relatively low levels of

Table 8 Complexity and heterogeneity of karyotypes

Cell lines	Tissue	Ploidy	SC ^a	NC	SH	NH
HCT-116	Colon	2				
CCRF-CEM	Leukemia	2				
HCT-15	Colon	2				
MOLT-4	Leukemia	4				
ACHN	Renal	2				
SR	Leukemia	2				
UO-31	Renal	2				
HCC-2998	Colon	2				
KM12	Colon	2				
NCI-H522	Lung	2				
A549/ATCC	Lung	3				
HL-60(TB)	Leukemia	2				
IGROV1	Ovarian	4				
UACC-257	Melanoma	3				
SW-620	Colon	2				
HT29	Colon	3				
SNB-75	CNS	2				
SK-OV-3	Ovarian	4				
T-47D	Breast	2				
DU-145	Prostate	3				
OVCAR-5	Ovarian	2				
LOX IMVI	Melanoma	3				
M14	Melanoma	3				
K-562	Leukemia	3				
UACC-62	Melanoma	3				
NCI-H460	Lung	2				
SNB-19	CNS	3				
MALME-3M	Melanoma	4				
CAKI-1	Renal	3				
COLO 205	Colon	3				
A498	Renal	3				
OVCAR-3	Ovarian	3				
MDA-MB-435	Breast	2				
MCF7	Breast	3				
RPMI-8226	Myeloma	3				
OVCAR-4	Ovarian	3				
OVCAR-8	Ovarian	2				
NCI-H226	Lung	3				
BT-549	Breast	3				
MDA-MB-231/ATCC	Breast	2				
786-0	Renal	4				
TK-10	Renal	4				
U251	CNS	2				
NCI-H322M	Lung	2				
NCI-H23	Lung	2				
HS 578T	Breast	3				
PC-3	Prostate	4				
SF-268	CNS	2				
SF-295	CNS	5				
SK-MEL-2	Melanoma	4				
SK-MEL-5	Melanoma	4				
HOP-62	Lung	4				
EKVX	Lung	3				
RXF-393	Renal	3				
SN12C	Renal	3				
HOP-92	Lung	4				
SK-MEL-28	Melanoma	4				
SF-539	CNS	4				

^a SC, structural complexity; NC, numerical complexity; SH, structural heterogeneity; NH, numerical heterogeneity; CNS, central nervous system. Green, low level (the lower 33%); orange, high level (upper 33%); and gray, intermediate level of parameters.

numerical and structural heterogeneity as well, although statistically significant differences were found only when comparing the levels of numerical, but not structural heterogeneity between MMR-defective and MMR-competent populations. Thus, karyotypic changes are widespread in the MMR-defective cell lines, but the number of these changes, in general, is relatively low. Low complexity and heteroge-

neity, however, are not specific defining characteristics of MMR-defective cell lines, because many MMR-competent cell lines share these features. This finding is supported by our previous results (15) showing that selected MMR-defective and MMR-competent cell lines can manifest similar levels of ongoing structural and numerical chromosomal instability.

Relationship between the NCI-60 and Primary Tumor Karyotypes. What is the relationship of the karyotypic findings in the NCI-60 cell lines to those that have been reported for primary tumors? Identification of common recurrent numerical changes across the whole NCI-60 panel revealed that the most frequent were losses of chromosomes 13, 21, and 22, and gains of chromosomes 5, 7, and 20. The two most frequent imbalances in the NCI-60 cell lines (gain of chromosome 7 and loss of 13) have been reported elsewhere as the most frequently observed chromosomal gain (7p arm +7q arm) and loss (13q arm) in 2210 solid tumors of 27 cancer types analyzed by comparative genomic hybridization (45). Moreover, chromosome copy number changes were concordant between the NCI-60 cell lines and these 2210 solid tumors for 19 chromosomes and discordant for only 4 (Y chromosome excluded). Tissue-specific combinations of chromosomal gains and losses found in our study also overlap with data obtained from large-scale analysis of G-banded karyotypes of solid tumors (46–48), and with chromosome copy number changes detected by comparative genomic hybridization or FISH in melanoma (49, 50), colon (45, 51), ovarian (52, 53), breast (54), lung, CNS, and renal (45) cancers. Given the observed and expected variation in karyotypes between one *versus* another individual tumor, it is striking that this significant overlap is found between primary tumors and this somewhat haphazardly collected set of lineage-related cell lines. This notion is supported by the finding that among the seven chromosomal bands involved in rearrangements in at least half of the NCI-60 ovarian cell lines, two of them were also among the most frequently rearranged in a series of 244 ovarian primary tumors (55). Additionally, the most frequent recurrent structural rearrangement in the NCI-60 lines (isochromosome 5p) was reported to represent a significant chromosomal change occurring with a fairly high frequency in a variety of cancers (20). This correlation suggests that the cell lines are relevant, not only to important issues of their own growth, development, evolution, and transformation, but to more generic issues of primary tumor formation and progression as well.

Structural Chromosomal Rearrangements and Breakpoint Analysis. Structural chromosomal rearrangements included translocations, deletions, insertions, inversions, duplications, HSRs, acentrics, minutes, and double minutes. Translocations and deletions were among the most frequent structural rearrangements.

The majority of translocations in the NCI-60 panel involved centromeric breakpoints. Rearrangements of chromosomes involving centromeric regions were encrypted into the signature karyotypes of many solid tumor cell lines and contributed to SH in some of them. In addition, centromeric chromosomal rearrangements led to numerical chromosomal changes and heterogeneity as well (as seen, for instance, from analysis of chromosome 13; Table 1 of Supplemental Data). Ninety percent of the hot spots of chromosomal rearrangement found in epithelial and other solid tumors, but not in leukemia/lymphoma cell lines, were localized to the centromeric regions of the chromosomes. This observation implies that centromeric chromosomal instability is one of the major factors leading to structural chromosomal rearrangements in cell lines derived from solid tumors, but not those derived from leukemias/lymphomas. Multiple whole-arm translocations have been reported for oral squamous cell carcinoma (56), squamous cell carcinoma of the skin (57), primary multiple myeloma (58), breast cancer cell lines (28), and prostate cancer cell lines (59). Isochromosomes and whole-arm JTs that are found to be common in solid tumors (20, 21) and cancer cell lines (19) can be products of this centromeric chromosomal instability.

Balanced and Unbalanced Translocations in the NCI-60 Cell Lines. Most of the translocations were unbalanced, as reported previously for epithelial tumors (21). However, balanced translocations were also found in our study. Perhaps surprisingly, cell lines with

balanced translocations were found with approximately the same frequency among leukemia and epithelial cancer cell lines. Balanced translocations have been particularly well characterized in leukemias and sarcomas, where they activate oncogenes through fusions with other genes or by dysregulation of transcription factors. In carcinomas, balanced reciprocal translocations have also been found (21), but they are considered to be rare events. This “rarity” may be due to technical reasons, such as difficulty in obtaining good metaphase spreads from epithelial cancer cells and the karyotypic complexity that has masked reciprocity when analyzed by standard G-banding techniques. Investigations based on new techniques (SKY and multi-color-FISH) allow better visualization of rearrangements in complex karyotypes, and delineation of unbalanced and balanced translocations. Karyotyping by multicolor-FISH of 15 breast tumor cell lines revealed the presence of balanced reciprocal translocations in 9 of them (34). Application of SKY to 9 ovarian adenocarcinoma cell lines and 4 primary tumors identified 7 reciprocal translocations in cell lines and 2 in primary tumors (35). Frequencies of balanced reciprocal translocations in these cases were 0.60 and 0.77 per breast and ovarian cancer cell line, respectively, and 0.5 balanced translocations per primary ovarian adenocarcinoma. Our experiments revealed similar frequencies of balanced reciprocal translocations (0.83 and 0.5 for breast and ovarian cancer cell lines, respectively). Reciprocal translocations may occur even more frequently because we detected the presence of nonclonal reciprocal derivatives matching clonal derivatives.

Both balanced and unbalanced translocations occur as a result of misrepair of double strand breaks (60), but precise mechanisms leading to unbalanced translocations remain obscure. It is plausible that unbalanced translocations can be, at least in part, products of reciprocal translocations. First, consistent losses of chromosomes due to numerical instability can lead to the eventual loss of one of reciprocal homologues. Second, reciprocal translocations can have different karyotypic consequences depending on the site of reciprocal exchange. They may lead to a balanced translocation with two derivatives, each containing a centromere. Reciprocal translocations can also create one derivative with two centromeres (dicentric), and another without a centromere (acentric; Fig. 4). Presence of dicentric chromosomes and acentric fragments in cancer cell lines indicates that this process, indeed, might take place. Dicentric chromosomes can be either stable or unstable, depending on the orientation of the kinetochore region of the chromatids joined by translocation. Therefore,

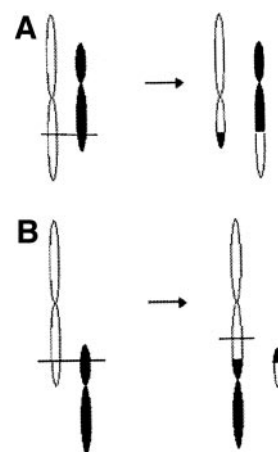


Fig. 4. Consequences of reciprocal translocations. A, “classical” reciprocal translocation forms two stable reciprocal derivatives. B, reciprocal exchange leads to formation of dicentric and acentric. During next mitotic division dicentric can be broken, triggering breakage-fusion-bridge cycles.

reciprocal translocations can lead to balanced and unbalanced rearrangements, and can be a source of both mitotically stable and unstable chromosomes. After the first mitotic division, unstable dicentric chromosomes can start breakage-fusion-bridge (BFB) cycles, originally described by McClintock (61), generate continuous variability of chromosome structure and lead to karyotypic heterogeneity. Evidence of frequent BFB cycles was found in malignancies that showed nonspecific chromosome aberrations but not in tumors with recurrent and highly specific aberrations, like Ewing's sarcoma (62, 63).

Telomere shortening and dysfunction is another process that can initiate BFB cycles (64, 65), nonreciprocal translocations (66), and evolution of complex chromosomal abnormalities in cancer cells (67). Similarly, loss of telomeres due to misrepair of near-telomeric double-strand breaks was also associated with BFB cycles and gross chromosomal rearrangements in yeast and mice (68–70). Our findings that terminal chromosomal bands were involved in 16% of translocations, and 30% of dicentric chromosomes were represented by telomeric fusions, support the notion that rearrangements involving telomeric or near-telomeric breakpoints make substantial contributions to karyotypic abnormalities.

As was mentioned above, the majority of translocations in the NCI-60 panel was represented by translocations involving centromeric breakpoints. Hypomethylation of centromeric and pericentromeric regions was observed in breast and ovarian cancer cells (71, 72). It was suggested that hypomethylation of these regions is an essential factor promoting cancer through effects on chromosomal stability (73). Recent investigations of the genomic structure of pericentromeric regions lead to the conclusion that these regions are often composed of inter- and intrachromosomally duplicated (paralogous) segments, predisposing to abnormal pairing and homologous recombination (74–76). Therefore, centromeric and pericentromeric regions can be major sites of inter- and intrachromosomal exchanges (at least, in many epithelial and other solid tumors), leading to balanced and unbalanced, mitotically stable, as well as unstable chromosomal rearrangements.

The delineation of the chromosomal complements of the cancer cell lines from the NCI-60 anticancer drug discovery panel allows subclassification of these cell lines based on their structural genome anatomy (ploidy, structural, and numerical chromosomal complexity and heterogeneity, and specific rearrangements). This dataset is already offering insights into the causes and consequences of genetic instability. It is one starting point for formation of hypotheses of destabilizing events that may occur during primary tumor development and either resolve or remain active in the cell line. It also provides a foundation for investigating associations between structural genome anatomy and cancer molecular markers and targets, gene expression, gene dosage, as well as resistance or sensitivity to tens of thousands of molecular compounds.

ACKNOWLEDGMENTS

We thank Patrick G. Moloney and James Miller for helping on the design of the website, Danny Wangsa for technical advice, Turid Knutsen and Hesus Padilla-Nash for advice in cytogenetic analysis, and W. Mihael Kuehl for critical reading of the manuscript.

GLOSSARY

Ploidy: the number of chromosomal sets present in a cell (*e.g.*, diploid = 2 sets).

Ploidy level (n): an approximation of ploidy for a cancer cell based on the modal number (m) of chromosomes in a tumor cell population; for the human, “n” is defined such that “m” falls within the range $23n \pm 11$.

Numerical complexity: deviations on the basis of centromere identification in the number of a specific chromosome from the established ploidy level.

Structural complexity: the number of different structurally rearranged chromosomes.

Clonal: present in two or more metaphases.

Nonclonal: present in one metaphase only.

Heterogeneity: metaphase-to-metaphase variations in a karyotypic parameter.

“Signature” karyotype: karyotypic features present in the majority of analyzed metaphases.

REFERENCES

- Shoemaker, R. H., Monks, A., Alley, M. C., Scudiero, D. A., Fine, D. L., McLemore, T. L., Abbott, B. J., Paull, K. D., Mayo, J. G., and Boyd, M. R. Development of human tumor cell line panels for use in disease-oriented drug screening. *Prog. Clin. Biol. Res.*, 276: 265–286, 1988.
- Monks, A., Scudiero, D., Skehan, P., Shoemaker, R., Paull, K., Vistica, D., Hose, C., Langley, J., Cronise, P., Vaigro-Wolff, A., *et al.* Feasibility of a high-flux anticancer drug screen using a diverse panel of cultured human tumor cell lines. *J. Natl. Cancer Inst.*, 83: 757–766, 1991.
- Monks, A., Scudiero, D. A., Johnson, G. S., Paull, K. D., and Sausville, E. A. The NCI anti-cancer drug screen: a smart screen to identify effectors of novel targets. *Anticancer Drug Des.*, 12: 533–541, 1997.
- Grever, M. R., Schepartz, S. A., and Chabner, B. A. The National Cancer Institute: cancer drug discovery and development program. *Semin. Oncol.*, 19: 622–638, 1992.
- Stinson, S. F., Alley, M. C., Kopp, W. C., Fiebig, H. H., Mullendore, L. A., Pittman, A. F., Kenney, S., Keller, J., and Boyd, M. R. Morphological and immunocytochemical characteristics of human tumor cell lines for use in a disease-oriented anticancer drug screen. *Anticancer Res.*, 12: 1035–1053, 1992.
- Bates, S. E., Fojo, A. T., Weinstein, J. N., Myers, T. G., Alvarez, M., Pauli, K. D., and Chabner, B. A. Molecular targets in the National Cancer Institute drug screen. *J. Cancer Res. Clin. Oncol.*, 121: 495–500, 1995.
- Weinstein, J. N., Kohn, K. W., Grever, M. R., Viswanadhan, V. N., Rubinstein, L. V., Monks, A. P., Scudiero, D. A., Welch, L., Koutsoukos, A. D., Chiusa, A. J., and *et al.* Neural computing in cancer drug development: predicting mechanism of action. *Science (Wash. DC)*, 258: 447–451, 1992.
- Weinstein, J. N., Myers, T. G., O'Connor, P. M., Friend, S. H., Fornace, A. J., Jr., Kohn, K. W., Fojo, T., Bates, S. E., Rubinstein, L. V., Anderson, N. L., Buolamwini, J. K., van Osdol, W. W., Monks, A. P., Scudiero, D. A., Sausville, E. A., Zaharevitz, D. W., Bunow, B., Viswanadhan, V. N., Johnson, G. S., Wittes, R. E., and Paull, K. D. An information-intensive approach to the molecular pharmacology of cancer. *Science (Wash. DC)*, 275: 343–349, 1997.
- O'Connor, P. M., Jackman, J., Bae, I., Myers, T. G., Fan, S., Mutoh, M., Scudiero, D. A., Monks, A., Sausville, E. A., Weinstein, J. N., Friend, S., Fornace, A. J., Jr., and Kohn, K. W. Characterization of the p53 tumor suppressor pathway in cell lines of the National Cancer Institute anticancer drug screen and correlations with the growth-inhibitory potency of 123 anticancer agents. *Cancer Res.*, 57: 4285–4300, 1997.
- Ross, D. T., Scherf, U., Eisen, M. B., Perou, C. M., Rees, C., Spellman, P., Iyer, V., Jeffrey, S. S., Van de Rijn, M., Waltham, M., Pergamenschikov, A., Lee, J. C., Lashkari, D., Shalon, D., Myers, T. G., Weinstein, J. N., Botstein, D., and Brown, P. O. Systematic variation in gene expression patterns in human cancer cell lines. *Nat. Genet.*, 24: 227–235, 2000.
- Scherf, U., Ross, D. T., Waltham, M., Smith, L. H., Lee, J. K., Tanabe, L., Kohn, K. W., Reinhold, W. C., Myers, T. G., Andrews, D. T., Scudiero, D. A., Eisen, M. B., Sausville, E. A., Pommier, Y., Botstein, D., Brown, P. O., and Weinstein, J. N. A gene expression database for the molecular pharmacology of cancer. *Nat. Genet.*, 24: 236–244, 2000.
- Staunton, J. E., Slonim, D. K., Collier, H. A., Tamayo, P., Angelo, M. J., Park, J., Scherf, U., Lee, J. K., Reinhold, W. O., Weinstein, J. N., Mesirov, J. P., Lander, E. S., and Golub, T. R. Chemosensitivity prediction by transcriptional profiling. *Proc. Natl. Acad. Sci. USA*, 98: 10787–10792, 2001.
- Modi, W. S., Nash, W. G., Ferrari, A. C., and O'Brien, S. J. Cytogenetic methodologies for gene mapping and comparative analyses in mammalian cell culture systems. *Gene Anal. Tech.*, 4: 75–85, 1987.
- Schröck, E., du Manoir, S., Veldman, T., Schoell, B., Wienberg, J., Ferguson-Smith, M. A., Ning, Y., Ledbetter, D. H., Bar-Am, I., Soenksen, D., Garini, Y., and Ried, T. Multicolor spectral karyotyping of human chromosomes [see comments]. *Science (Wash. DC)*, 273: 494–497, 1996.
- Roschke, A. V., Stover, K., Tonon, G., Schaffer, A. A., and Kirsch, I. R. Stable karyotypes in epithelial cancer cell lines despite high rates of ongoing structural and numerical chromosomal instability. *Neoplasia*, 4: 19–31, 2002.
- Mitelman, F. (Ed.) *ISCN (1995): An International System for Human Cytogenetic Nomenclature*. Basel: S. Karger, 1995.
- Tonon, G., Roschke, A., Stover, K., Shou, Y., Kuehl, W. M., and Kirsch, I. R. Spectral karyotyping combined with locus-specific FISH simultaneously defines genes and chromosomes involved in chromosomal translocations. *Genes Chromosomes Cancer*, 27: 418–423, 2000.
- Kirsch, I. R., Green, E. D., Yonescu, R., Strausberg, R., Carter, N., Bentley, D., Leversha, M. A., Dunham, I., Braden, V. V., Hilgenfeld, E., Schuler, G., Lash, A. E., Shen, G. L., Martelli, M., Kuehl, W. M., Klausner, R. D., and Ried, T. A systematic,

- high-resolution linkage of the cytogenetic and physical maps of the human genome. *Nat. Genet.*, *24*: 339–340, 2000.
19. Padilla-Nash, H. M., Heselmeyer-Haddad, K., Wangsa, D., Zhang, H., Ghadimi, B. M., Macville, M., Augustus, M., Schröck, E., Hilgenfeld, E., and Ried, T. Jumping translocations are common in solid tumor cell lines and result in recurrent fusions of whole chromosome arms. *Genes Chromosomes Cancer*, *30*: 349–363, 2001.
 20. Atkin, N. B., and Baker, M. C. Small metacentric marker chromosomes, particularly isochromosomes, in cancer. *Hum Genet*, *79*: 96–102, 1988.
 21. Mitelman, F., Johansson, B., and Mertens, F. (Eds.) *Mitelman Database of Chromosome Aberrations in Cancer*, <http://cgap.nci.nih.gov/Chromosomes/Mitelman>, 2003.
 22. Taverna, P., Liu, L., Hanson, A. J., Monks, A., and Gerson, S. L. Characterization of MLH1 and MSH2 DNA mismatch repair proteins in cell lines of the NCI anticancer drug screen. *Cancer Chemother. Pharmacol.*, *46*: 507–516, 2000.
 23. Ohzeki, S., Tachibana, A., Tatsumi, K., and Kato, T. Spectra of spontaneous mutations at the hprt locus in colorectal carcinoma cell lines defective in mismatch repair. *Carcinogenesis (Lond.)*, *18*: 1127–1133, 1997.
 24. Aurich-Costa, J., Vannier, A., Gregoire, E., Nowak, F., and Cherif, D. IPM-FISH, a new M-FISH approach using IRS-PCR painting probes: application to the analysis of seven human prostate cell lines. *Genes Chromosomes Cancer*, *30*: 143–160, 2001.
 25. Davidson, J. M., Gorringer, K. L., Chin, S. F., Orsetti, B., Besret, C., Courtney-Cahen, C., Roberts, I., Theillet, C., Caldas, C., and Edwards, P. A. Molecular cytogenetic analysis of breast cancer cell lines. *Br. J. Cancer*, *83*: 1309–1317, 2000.
 26. Gribble, S. M., Roberts, I., Grace, C., Andrews, K. M., Green, A. R., and Nacheva, E. P. Cytogenetics of the chronic myeloid leukemia-derived cell line K562: karyotype clarification by multicolor fluorescence *in situ* hybridization, comparative genomic hybridization, and locus-specific fluorescence *in situ* hybridization. *Cancer Genet. Cytogenet.*, *118*: 1–8, 2000.
 27. Kawai, K., Viars, C., Arden, K., Tarin, D., Urquidí, V., and Goodison, S. Comprehensive karyotyping of the HT-29 colon adenocarcinoma cell line. *Genes Chromosomes Cancer*, *34*: 1–8, 2002.
 28. Kytölä, S., Rummukainen, J., Nordgren, A., Karhu, R., Farnebo, F., Isola, J., and Larsson, C. Chromosomal alterations in 15 breast cancer cell lines by comparative genomic hybridization and spectral karyotyping. *Genes Chromosomes Cancer*, *28*: 308–317, 2000.
 29. Lu, Y. J., Morris, J. S., Edwards, P. A., and Shipley, J. Evaluation of 24-color multifluor-fluorescence *in-situ* hybridization (M-FISH) karyotyping by comparison with reverse chromosome painting of the human breast cancer cell line T-47D. *Chromosome Res.*, *8*: 127–132, 2000.
 30. Luk, C., Tsao, M. S., Bayani, J., Shepherd, F., and Squire, J. A. Molecular cytogenetic analysis of non-small cell lung carcinoma by spectral karyotyping and comparative genomic hybridization. *Cancer Genet. Cytogenet.*, *125*: 87–99, 2001.
 31. Masramon, L., Ribas, M., Cifuentes, P., Arribas, R., García, F., Egozcue, J., Peinado, M. A., and Miró, R. Cytogenetic characterization of two colon cell lines by using conventional G-banding, comparative genomic hybridization, and whole chromosome painting. *Cancer Genet. Cytogenet.*, *121*: 17–21, 2000.
 32. Melcher, R., Koehler, S., Steinlein, C., Schmid, M., Mueller, C. R., Luehrs, H., Menzel, T., Scheppach, W., Moerk, H., Scheurlen, M., Koehle, J., and Al-Taie, O. Spectral karyotype analysis of colon cancer cell lines of the tumor suppressor and mutator pathway. *Cytogenet. Genome Res.*, *98*: 22–28, 2002.
 33. Pan, Y., Lui, W. O., Nupponen, N., Larsson, C., Isola, J., Visakorpi, T., Bergerheim, U. S., and Kytölä, S. 5q11, 8p11, and 10q22 are recurrent chromosomal breakpoints in prostate cancer cell lines. *Genes Chromosomes Cancer*, *30*: 187–195, 2001.
 34. Popovici, C., Basset, C., Bertucci, F., Orsetti, B., Adélaide, J., Mozziconacci, M. J., Conte, N., Murati, A., Ginestier, C., Charafe-Jauffret, E., Ethier, S. P., Lafage-Pochitaloff, M., Theillet, C., Birnbaum, D., and Chaffanet, M. Reciprocal translocations in breast tumor cell lines: cloning of a t(3;20) that targets the FHIT gene. *Genes Chromosomes Cancer*, *35*: 204–218, 2002.
 35. Rao, P. H., Harris, C. P., Yan Lu, X., Li, X. N., Mok, S. C., and Lau, C. C. Multicolor spectral karyotyping of serous ovarian adenocarcinoma. *Genes Chromosomes Cancer*, *33*: 123–132, 2002.
 36. Strefford, J. C., Lillington, D. M., Young, B. D., and Oliver, R. T. The use of multicolor fluorescence technologies in the characterization of prostate carcinoma cell lines: a comparison of multiplex fluorescence *in situ* hybridization and spectral karyotyping data. *Cancer Genet. Cytogenet.*, *124*: 112–121, 2001.
 37. Varela-García, M., Boomer, T., and Miller, G. J. Karyotypic similarity identified by multiplex-FISH relates four prostate adenocarcinoma cell lines: PC-3, PPC-1, ALVA-31, and ALVA-41. *Genes Chromosomes Cancer*, *31*: 303–315, 2001.
 38. Mitelman, F., Johansson, B., and Mertens, F. *Catalog of chromosome aberrations in cancer*, Ed. 5, p. 2 v. (xxix, 4252). New York: Wiley-Liss, 1994.
 39. Johansson, B., Mertens, F., and Mitelman, F. Primary vs. secondary neoplasia-associated chromosomal abnormalities—balanced rearrangements vs. genomic imbalances?. *Genes Chromosomes Cancer*, *16*: 155–163, 1996.
 40. Chen, T. R., Drabkowski, D., Hay, R. J., Macy, M., and Peterson, W., Jr. WiDr is a derivative of another colon adenocarcinoma cell line, HT-29. *Cancer Genet. Cytogenet.*, *27*: 125–134, 1987.
 41. Macville, M., Schrock, E., Padilla-Nash, H., Keck, C., Ghadimi, B. M., Zimonjic, D., Popescu, N., and Ried, T. Comprehensive and definitive molecular cytogenetic characterization of HeLa cells by spectral karyotyping. *Cancer Res.*, *59*: 141–150, 1999.
 42. Knutsen, T. V., Rao, K., Ried, T., Mickle, L., Schneider, E., Miyake, K., Ghadimi, M., Padilla-Nash, H., Pack, S., Greenberger, L., Cowan, K., Dean, M., Fojo, T., and Bates, S. Amplification of 4q21–q22 and the MXR gene in independently derived mitoxantrone-resistant cell lines. *Genes Chromosomes Cancer*, *27*: 110–116, 2000.
 43. Reinhold, W. C., Kouros-Mehr, H., Kohn, K. W., Maunakea, A. K., Lababidi, S., Roschke, A., Stover, K., Alexander, J., Pantazis, P., Miller, L., Liu, E., Kirsch, I. R., Urasaki, Y., Pommier, Y., and Weinstein, J. N. Apoptotic susceptibility of cancer cells selected for camptothecin resistance: gene expression profiling, functional analysis, and molecular interaction mapping. *Cancer Res.*, *63*: 1000–1011, 2003.
 44. Fabarius, A., Hehlmann, R., and Duesberg, P. H. Instability of chromosome structure in cancer cells increases exponentially with degrees of aneuploidy. *Cancer Genet. Cytogenet.*, *143*: 59–72, 2003.
 45. Rooney, P. H., Murray, G. I., Stevenson, D. A., Haites, N. E., Cassidy, J., and McLeod, H. L. Comparative genomic hybridization and chromosomal instability in solid tumours. *Br. J. Cancer*, *80*: 862–873, 1999.
 46. Mitelman, F., Johansson, B., Mandahl, N., and Mertens, F. Clinical significance of cytogenetic findings in solid tumors. *Cancer Genet. Cytogenet.*, *95*: 1–8, 1997.
 47. Höglund, M., Gisselsson, D., Mandahl, N., Johansson, B., Mertens, F., Mitelman, F., and Sall, T. Multivariate analyses of genomic imbalances in solid tumors reveal distinct and converging pathways of karyotypic evolution. *Genes Chromosomes Cancer*, *31*: 156–171, 2001.
 48. Höglund, M., Gisselsson, D., Hansen, G. B., Säll, T., and Mitelman, F. Multivariate analysis of chromosomal imbalances in breast cancer delineates cytogenetic pathways and reveals complex relationships among imbalances. *Cancer Res.*, *62*: 2675–2680, 2002.
 49. Bastian, B. C., LeBoit, P. E., Hamm, H., Brocker, E. B., and Pinkel, D. Chromosomal gains and losses in primary cutaneous melanomas detected by comparative genomic hybridization. *Cancer Res.*, *58*: 2170–2175, 1998.
 50. Balázs, M., Ádám, Z., Treszl, A., Bégány, A., Hunyadi, J., and Ádány, R. Chromosomal imbalances in primary and metastatic melanomas revealed by comparative genomic hybridization. *Cytometry*, *46*: 222–232, 2001.
 51. Ried, T., Knutzen, R., Steinbeck, R., Blegen, H., Schröck, E., Heselmeyer, K., du Manoir, S., and Auer, G. Comparative genomic hybridization reveals a specific pattern of chromosomal gains and losses during the genesis of colorectal tumors. *Genes Chromosomes Cancer*, *15*: 234–245, 1996.
 52. Jenkins, R. B., Bartelt, D., Jr., Stalboerger, P., Persons, D., Dahl, R. J., Podratz, K., Keeney, G., and Hartmann, L. Cytogenetic studies of epithelial ovarian carcinoma. *Cancer Genet. Cytogenet.*, *71*: 76–86, 1993.
 53. Blegen, H., Einhorn, N., Sjövall, K., Roschke, A., Ghadimi, B. M., McShane, L. M., Nilsson, B., Shah, K., Ried, T., and Auer, G. Prognostic significance of cell cycle proteins and genomic instability in borderline, early and advanced stage ovarian carcinomas. *Int. J. Gynecol. Cancer*, *10*: 477–487, 2000.
 54. Teixeira, M. R., Pandis, N., and Heim, S. Cytogenetic clues to breast carcinogenesis. *Genes Chromosomes Cancer*, *33*: 1–16, 2002.
 55. Taetle, R., Aickin, M., Yang, J. M., Panda, L., Emerson, J., Roe, D., Adair, L., Thompson, F., Liu, Y., Wisner, L., Davis, J. R., Trent, J., and Alberts, D. S. Chromosome abnormalities in ovarian adenocarcinoma: I. Nonrandom chromosome abnormalities from 244 cases. *Genes Chromosomes Cancer*, *25*: 290–300, 1999.
 56. Hermesen, M. A., Joenje, H., Arwert, F., Welters, M. J., Braakhuis, B. J., Bagnay, M., Westerveld, A., and Slater, R. Centromeric breakage as a major cause of cytogenetic abnormalities in oral squamous cell carcinoma. *Genes Chromosomes Cancer*, *15*: 1–9, 1996.
 57. Jin, Y., Martins, C., Jin, C., Salemark, L., Jonsson, N., Persson, B., Roque, L., Fonseca, I., and Wennerberg, J. Nonrandom karyotypic features in squamous cell carcinomas of the skin. *Genes Chromosomes Cancer*, *26*: 295–303, 1999.
 58. Sawyer, J. R., Lukacs, J. L., Thomas, E. L., Swanson, C. M., Goosen, L. S., Sammartino, G., Gilliland, J. C., Munshi, N. C., Tricot, G., Shaughnessy, J. D., Jr., and Barlogie, B. Multicolor spectral karyotyping identifies new translocations and a recurring pathway for chromosome loss in multiple myeloma. *Br. J. Haematol.*, *112*: 167–174, 2001.
 59. Beheshti, B., Park, P. C., Sweet, J. M., Trachtenberg, J., Jewett, M. A., and Squire, J. A. Evidence of chromosomal instability in prostate cancer determined by spectral karyotyping (SKY) and interphase fish analysis. *Neoplasia*, *3*: 62–69, 2001.
 60. Richardson, C., and Jasin, M. Frequent chromosomal translocations induced by DNA double-strand breaks. *Nature (Lond.)*, *405*: 697–700, 2000.
 61. McClintock, B. The stability of broken ends of chromosomes in *Zea mays*. *Genetics*, *26*: 234–282, 1940.
 62. Gisselsson, D., Pettersson, L., Höglund, M., Heidenblad, M., Gorunova, L., Wiegant, J., Mertens, F., Dal Cin, P., Mitelman, F., and Mandahl, N. Chromosomal breakage-fusion-bridge events cause genetic intratumor heterogeneity. *Proc. Natl. Acad. Sci. USA*, *97*: 5357–5362, 2000.
 63. Saunders, W. S., Shuster, M., Huang, X., Gharaiheb, B., Enyenihi, A. H., Petersen, I., and Gollin, S. M. Chromosomal instability and cytoskeletal defects in oral cancer cells. *Proc. Natl. Acad. Sci. USA*, *97*: 303–308, 2000.
 64. Artandi, S. E., and DePinho, R. A. A critical role for telomeres in suppressing and facilitating carcinogenesis. *Curr. Opin. Genet. Dev.*, *10*: 39–46, 2000.
 65. Rudolph, K. L., Millard, M., Bosenberg, M. W., and DePinho, R. A. Telomere dysfunction and evolution of intestinal carcinoma in mice and humans. *Nat. Genet.*, *28*: 155–159, 2001.
 66. Artandi, S. E., Chang, S., Lee, S. L., Alson, S., Gottlieb, G. J., Chin, L., and DePinho, R. A. Telomere dysfunction promotes non-reciprocal translocations and epithelial cancers in mice. *Nature (Lond.)*, *406*: 641–645, 2000.
 67. Gisselsson, D., Jonson, T., Petersen, A., Strombeck, B., Dal Cin, P., Höglund, M., Mitelman, F., Mertens, F., and Mandahl, N. Telomere dysfunction triggers extensive DNA fragmentation and evolution of complex chromosome abnormalities in human malignant tumors. *Proc. Natl. Acad. Sci. USA*, *98*: 12683–12688, 2001.
 68. Myung, K., Chen, C., and Kolodner, R. D. Multiple pathways cooperate in the

- suppression of genome instability in *Saccharomyces cerevisiae*. *Nature (Lond.)*, *411*: 1073–1076, 2001.
69. Myung, K., Datta, A., and Kolodner, R. D. Suppression of spontaneous chromosomal rearrangements by S phase checkpoint functions in *Saccharomyces cerevisiae*. *Cell*, *104*: 397–408, 2001.
70. Lo, A. W., Sprung, C. N., Fouladi, B., Pedram, M., Sabatier, L., Ricoul, M., Reynolds, G. E., and Murnane, J. P. Chromosome instability as a result of double-strand breaks near telomeres in mouse embryonic stem cells. *Mol. Cell. Biol.*, *22*: 4836–4850, 2002.
71. Narayan, A., Ji, W., Zhang, X. Y., Marrogi, A., Graff, J. R., Baylin, S. B., and Ehrlich, M. Hypomethylation of pericentromeric DNA in breast adenocarcinomas. *Int. J. Cancer*, *77*: 833–838, 1998.
72. Qu, G., Dubeau, L., Narayan, A., Yu, M. C., and Ehrlich, M. Satellite DNA hypomethylation vs. overall genomic hypomethylation in ovarian epithelial tumors of different malignant potential. *Mutat. Res.*, *423*: 91–101, 1999.
73. Eden, A., Gaudet, F., Waghmare, A., and Jaenisch, R. Chromosomal instability and tumors promoted by DNA hypomethylation. *Science (Wash. DC)*, *300*: 455, 2003.
74. Eichler, E. E. Masquerading repeats: paralogous pitfalls of the human genome. *Genome Res.*, *8*: 758–762, 1998.
75. Bailey, J. A., Yavor, A. M., Massa, H. F., Trask, B. J., and Eichler, E. E. Segmental duplications: organization and impact within the current human genome project assembly. *Genome Res.*, *11*: 1005–1017, 2001.
76. Horvath, J. E., Bailey, J. A., Locke, D. P., and Eichler, E. E. Lessons from the human genome: transitions between euchromatin and heterochromatin. *Hum. Mol. Genet.*, *10*: 2215–2223, 2001.